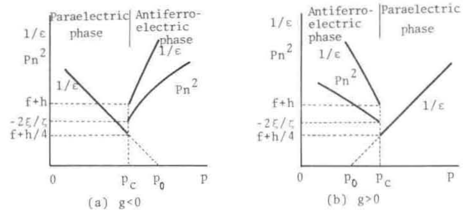

Fig. 4. First order transition with pressure (no applied field).

(4), the reciprocal of the permittivity is

$$1/\varepsilon=3f-2(u+gp)+(4h/3)\{1+\sqrt{1+3(f-u-gp)/2h}\}. \quad (23)$$

The permittivity at p_c in the paraelectric phase ε_{cp} and the permittivity at p_c in the antiferroelectric phase ε_{ca} are obtained by putting p_c given by eq. (21) into p in eqs. (5) and (23) respectively, so the ratio K of ε_{cp} to ε_{ca} is

$$K=\varepsilon_{cp}/\varepsilon_{ca}=(1+h/f)/(1+h/4f). \quad (24)$$

The schematic pressure dependences of $1/\varepsilon$ and P_n^2 for the first order transition are shown in Fig. 4(a) and (b). Figure 4(a) corresponds to the transition from the paraelectric phase to the antiferroelectric phase with increasing pressure, and Fig. 4(b) corresponds to the transition from the antiferroelectric phase to the paraelectric phase.

(ii) Under bias field; In this case, $P_m\neq 0$ and $P_n\neq 0$ under the electric field E. Then, relations [F vs. P_m], [E vs. P_m] and [$1/\varepsilon$ vs. E] are obtained analytically or numerically by putting P_n^2 in eq. (3.b) into P_n^2 in eqs. (2)–(4).

(iii) Under strong bias field; As in the case of the second order transition, at the moment E exceeded a critical value E_a, the state changes from the antiferroelectric phase to the induced phase. In this phase, $P_m\neq 0$ and $P_n=0$.

So, from eqs. (3.a), (4) and (2), the relations [E vs. P_m], [E vs. ε] and [F vs. P_m] are

$$E=\frac{1}{2}(u+gp+f+\xi P_m^2+3\zeta P_m^4/8)P_m \quad (25)$$

$$E=\frac{1}{5}\left[2(u+gp+f)+\frac{1}{\varepsilon}-\frac{4}{5}h\left\{1+\sqrt{1-5\left(u+gp+f-\frac{2}{\varepsilon}\right)/6h}\right\}\right]\times\sqrt{-\frac{4\xi}{5\zeta}\left\{1+\sqrt{1-5\left(u+gp+f-\frac{2}{\varepsilon}\right)/6h}\right\}} \quad (26)$$

$$W\equiv F-\frac{1}{2}cp^2=-\frac{1}{4}\left(u+gp+f+\frac{3}{2}\xi P_m^2+\frac{5}{8}\zeta P_m^4\right)P_m^2. \quad (27)$$

Analytical results for antiferroelectrics of the first order transition obtained numerically by putting $u=9.48\times 10^8$ m/F, $g=-5.62\times 10^7$ m/F·kbar, $f=2.08\times 10^8$ m/F, $\xi=-3.31\times 10^{11}$ m^5/F·C^2 and $\zeta=2.65\times 10^{14}$ m^9/F·C^4 [6] into eqs. (22), (23) and (25), etc. are as follows; (1) Double hysteresis loops like Fig. 2 are obtained between the electric field and the polarization under various pressures ($p=13$, 15 and 18 kbar). The critical field E_a seen in a loop increases with increasing pressure at a given temperature, while E_a increases with decreasing temperature at atmospheric pressure.[7] (2) The electric field dependence of the relative permittivity ε_r under various pressures ($p=13$, 15 and 18 kbar) is similar to Fig. 3(b), and is, in the antiferroelectric phase, qualitatively compatible with Okada's experimental result at atmospheric pressure.[8]

§3. Application of the Analysis to the Experimental Result

This analysis was applied to the experimental result for polycrystalline Pb_2MgWO_6 belonging to the type of Fig. 4(b). Solid lines in Fig. 5 show the pressure dependences of the reciprocal of the relative permittivity $1/\varepsilon_r$ under various temperatures measured by Polandov,[3] and $1/\varepsilon_r$ increases linearly with pressure in the paraelectric phase (above $p_c=1.14$ kbar). From

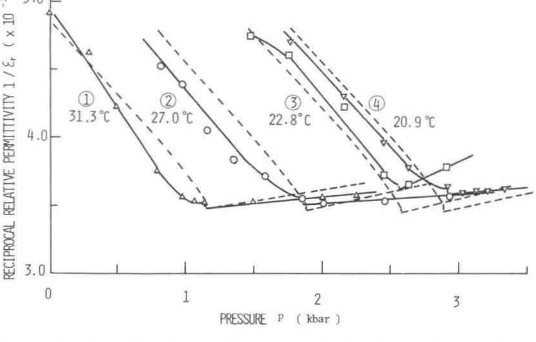

Fig. 5. Application of the analytical result to the experimental result for antiferroelectric Pb_2MgWO_6 belonging to the first order transition (after Polandov).

the curve ① in Fig. 5, the slope of $1/\varepsilon$ to p in the paraelectric phase $g=5.32\times10^7$ m/F·kbar, the characteristic pressure $p_o=-13.7$ kbar and $K=3.52/3.48=1.01$ are found. By substituting this value of K for eq. (24), $h/f=0.016$. By substituting the above values for eq. (21), $f=3.93\times10^8$ m/F and $h=6.29\times10^6$ m/F.

According to Polandov, the temperature (T) dependence of p_c is $p_c=\alpha-\beta T$, where $\alpha=$ 6.34 kbar and $\beta=1.66\times10^{-1}$ kbar/°C. By elimination of p_c from this equation and eq. (21), and by substitution of $C(T-T_1)$ for u in eq. (21) (because Curie-Weiss' law is satisfied), $C=$ 8.80×10^6 m/F·°C and $T_1=-6.32$°C.

The dotted lines in Fig. 5 show the pressure dependences of $1/\varepsilon_r$ under various temperatures in the paraelectric phase and the antiferroelectric phase calculated by putting all the estimated constants into eqs. (5) and (23), and agree approximately with the solid lines which show measured values.

§4. Conclusion

By applying the Kittel's antiferroelectric model and the Cross' polarizations to the free energy function for ferroelectrics under hydrostatic pressure, the Gibbs function for antiferroelectrics under hydrostatic pressure was given in terms of pressure, polarization and electric field. And antiferroelectric phenomena such as the Curie-Weiss' law on pressure in the paraelectric phase, pressure dependence of the permittivity or the spontaneous polarization in the antiferroelectric phase, electric field dependence of the permittivity and double hysteresis loops under various pressures could be successfully explained on the basis of this energy function.

The analytical results were applied to the experimental results not only for Pb_2MgWO_6, but also for $PbZrO_3$[9] reported by Samara and $Cu(HCOO)_2\cdot4H_2O$ reported recently by authors,[6] and were confirmed to be useful to explain antiferroelectric phenomena under hydrostatic pressure.

References

1) C. Kittel: Phys. Rev. **82** (1951) 729.
2) A. F. Devonshire: Phil. Mag. **40** (1949) 1040; *ibid.* **42** (1951) 1065.
3) I. N. Polandov: Soviet Phys. Solid State **5** (1963) 838.
4) S. Fujimoto and N. Yasuda: Trans. I. E. E. Japan **93-A** (1973) 361 [in Japanese].
5) L. E. Cross: J. Phys. Soc. Japan **23** (1967) 77.
6) S. Fujimoto, N. Yasuda and H. Ukai: *Proc. of the I.E.E.E. Symp. on Applications of Ferroelectrics 1975*, Ferroelectrics **10** (1976) 96.
7) K. Okada and H. Sugie: J. Phys. Soc. Japan **25** (1968) 1128.
8) K. Okada, M. I. Kay, D. T. Cromer and I. Almodovar: J. chem. Phys. **44** (1966) 1648.
9) G. A. Samara: Phys. Rev. **1** (1970) 3777.